




Dynamic screening and two-center effects in neutral and partially dressed ion-atom collisionsN. J. Esponda ^{1,*}, M. A. Quinto ¹, R. D. Rivarola,^{1,2} and J. M. Monti ^{1,2}¹*Grupo de Colisiones Atómicas IFIR-CONICET, Rosario CP2000, Argentina*²*Laboratorio de Colisiones Atómicas FCEIA-UNR, Rosario CP2000, Argentina* (Received 21 October 2021; revised 11 February 2022; accepted 8 March 2022; published 23 March 2022)

In collisions involving projectiles with bound electrons, partial or total screening of their nuclear charge must be considered. Accordingly, a projectile dynamic effective charge, as a function of the collision momentum transfer, is included in the state-of-the-art continuum distorted wave with eikonal initial state model. This correction, applied in the exit channel, recovers a two-center description from collisions with neutral projectiles. Also, an improvement of both target and projectile ionization double differential cross sections is achieved, especially at the binary encounter and electron capture to the continuum peaks. The results calculated by our analytical model are shown in accordance with previous theoretical and experimental work.

DOI: [10.1103/PhysRevA.105.032817](https://doi.org/10.1103/PhysRevA.105.032817)**I. INTRODUCTION**

The study of electron emission in atomic collisions becomes considerably more complex by the presence of bound electrons in ionic or atomic projectiles. In comparison with the impact of the bare atomic nucleus, some aspects behave in a similar manner, others may change, and some new characteristics in the differential cross section spectra can arise.

Broadly speaking, the interaction between the projectile electronic structure and the target active electron can be classified as mono-electronic or dielectronic [1,2]. In the former, the projectile electrons play a passive role by screening the nuclear field, so the target active electron is basically interacting with a screened nucleus [3]. On the other hand, in the dielectronic interaction the projectile electrons assume an active role, thereby being excited to a discrete or continuum state simultaneously with target ionization [4].

Under the first Born approximation and therefore for high-energy collisions, DuBois and Manson [2,3] show that dielectronic interactions contribute principally to the low-energy electron emission. However, it can give a significant contribution under a certain transferred momentum threshold, which depends on the projectile nuclear charge and its ionization state. Additionally, Manson and Toburen [5] analyzed the screening effects over the double differential cross section (DDCS) for He ionization by the impact of He⁺ ions. They found that for a small momentum transfer the DDCS behaves as if the projectile were a bare H⁺ nucleus, i.e., the screening in He⁺ is complete for distant collisions. In contrast, for larger momentum transfer, e.g., binary collision, the He ionization DDCS is similar to the one calculated for the impact of bare He²⁺ projectiles; in other words, there is no screening at all.

Generally, two-center emission effects are relevant in the intermediate emission energy spectrum. A clear example is

the electron capture to the continuum (ECC) cusp composed by electrons emitted at approximately 0° with velocities similar to that of the projectile. This phenomenon is commonly interpreted as if the emitted electron remains in a low-energy scattering state of the active electron-projectile system. In principle, this interpretation relies on the presence of long-range interactions. However, Garibotti and Barrachina [6] have predicted theoretically the presence of a similar cusp considering different screening potentials for ionic projectiles. The first clear experimental evidence that the ECC cusp also occurs in collisions involving neutral projectiles was obtained by Sarkadi *et al.* [7] using He projectiles. Various theoretical works have elaborated some explanations for the ECC cusp formation under a total absence of long-range interactions. For example, Jakubaša-Amundsen [8] proposed that the cusp might be a consequence of short-range interactions, while Barrachina [9] indicated that the cusp might be produced by a low-lying virtual state resonance between the electron and the excited He projectile. This last formulation has been demonstrated to be greatly precise and accurate to explain a vast variety of experimental measurements [10] performed with He projectiles, especially those in [11,12] where the fraction of He metastable states of the beam was controlled.

In the present paper we include an effective projectile screening into the actual, single-ionization, continuum distorted wave with eikonal initial state (CDW-EIS) [13–15] model. Previous works have already extended the CDW-EIS model to the case of partially dressed ions [16–19]. In that extension, the projectile distortions were defined by its net charge and therefore the model loses its two-center description if neutral projectiles were involved, e.g., when calculating the projectile electron loss. Therefore, we propose the use of a dynamic effective charge to take into account the screening of dressed projectiles as a continuous function of the momentum transfer, recovering two-center emission effects.

In Sec. II we present the CDW-EIS *prior* model for dressed projectiles and develop the expression for the projectile dynamic effective charge. In Sec. III A we use

*esponda@ifir-conicet.gov.ar

physical arguments in favor of using the dynamic charge only in the final channel. Then, in Sec. III B we discuss the similarities and differences between our calculations and those of Manson and Toburen [5] for target ionization by structured particles. In Sec. III C we show our results for ECC not only for target ionization by neutral atom impact but also for projectile ionization, which is significant for backscattering emission as shown in Sec. III D. Atomic units are used unless otherwise stated.

II. THEORY

Let us study first the single ionization of a target atom in a collision with an incident projectile which carries some bound electrons. This multielectronic system can be rather simplified under the independent electron model, which assumes that the nonionized electrons remain frozen in their initial states during the collision. These electrons are called the *passive* ones, whereas the electron being ejected from the target is referred to as the *active* electron. Then, the one-electron Hamiltonian in the laboratory reference frame is given by

$$H_{\text{el}} = -\frac{1}{2}\nabla_r^2 + V_T(\mathbf{x}) + V_P(\mathbf{s}) + V_s(\mathbf{R}), \quad (1)$$

where \mathbf{x} and \mathbf{s} are the positions of the active electron relative to the target and projectile nucleus, respectively. In addition, $V_T(\mathbf{x})$ is the target potential while $V_P(\mathbf{s})$ is the interaction between the active electron and the screened projectile. The $V_s(\mathbf{R})$ term contains the mean interaction of the projectile with the target nucleus and passive electrons, so it only depends on the internuclear coordinate \mathbf{R} . However, regarding the straight-line version of the impact parameter approximation, V_s contributes to the transition amplitude with a global phase factor which does not affect the physical predictions for double, simple, or total cross-section calculations [20], so it will be ignored henceforth.

As it is well known, the continuum distorted-wave (CDW) approach takes the projectile-active electron interaction as a perturbation, thereby proposing a distortion factor $\mathcal{L}(s)_{i,f}^{+,-}$ to the initial bound and final continuum target-electron eigenstates. Thus,

$$\chi_i^+(\mathbf{r}, t) = \psi_i(\mathbf{x}, t)\mathcal{L}_i^+(\mathbf{s}), \quad (2a)$$

$$\chi_f^-(\mathbf{r}, t) = \psi_f(\mathbf{x}, t)\mathcal{L}_f^-(\mathbf{s}) \quad (2b)$$

are the initial and final channel distorted-wave functions.

It must be said that calculating the exact continuum states for dressed ions or atoms is a quite time-consuming computational task. Instead, we may use the analytical hydrogenic continuum factors defining an effective nuclear charge for both target and projectile. For $\mathcal{L}_i^+(\mathbf{s})$ we may take its high-energy and asymptotic limit, the so-called eikonal initial-state approximation, to avoid the known divergences arising in the CDW when this limit is not taken [21]. Therefore the distortions are chosen as

$$\mathcal{L}_i^+(\mathbf{s}) = \exp[-iv \ln(vs + \mathbf{v} \cdot \mathbf{s})], \quad (3a)$$

$$\mathcal{L}_f^-(\mathbf{s}) = N^*(\xi) {}_1F_1[-i\xi, 1, -i(ps + \mathbf{p} \cdot \mathbf{s})] \quad (3b)$$

where ${}_1F_1$ is the confluent hypergeometric function, $N(\xi) = \Gamma(1 - i\xi) \exp(\pi\xi/2)$ is its normalization factor, \mathbf{v} is the projectile velocity, $\mathbf{p} = \mathbf{k} - \mathbf{v}$ is the momentum of the ejected

electron in the projectile frame, \mathbf{k} is the ejected electron momentum in the target reference frame, and $v = Z_p^{\text{eff}}/v$ and $\xi = Z_p^{\text{eff}}/p$ for some effective projectile nuclear charge Z_p^{eff} .

So far, for a projectile with N bounded electrons and Z_p protons, the asymptotic net charge $q = Z_p - N$ was taken as the effective charge Z_p^{eff} . However, in collisions with neutral projectiles, $q = 0$ and then $\mathcal{L}(s)_{i,f}^{+,-} = 1$. In other words, the distortions (3a) and (3b) will vanish. As a consequence, the ionization amplitude (6) will be given only by the short-range part of the projectile potential (7), as in a first Born approximation.

In CDW-EIS, although taking $q = Z_p - N$ might be reasonable if the impact parameter is so large that the nuclear charge Z_p gets completely screened by its bounded electrons, for smaller impact parameters the field produced by Z_p could be partially screened or not screened at all.

Within the first Born approximation formalism, when a dressed projectile is considered, its effective charge turns out to depend on the momentum transfer \mathbf{K} . This dependence involves the projectile form factor $F(\mathbf{K})$ [2,22]. Provided that the projectile remains in its fundamental state throughout the collision, the effective charge is [3]

$$q_K = Z_p - F(\mathbf{K}), \quad (4)$$

where $F(\mathbf{K})$ for the ground state $\phi_{Pi}(\mathbf{r}_1, \mathbf{r}_2, \dots, \mathbf{r}_N)$ of the N -electron projectile is given by

$$F(\mathbf{K}) = \left\langle \phi_{Pi} \left| \sum_{j=1}^N e^{i\mathbf{K} \cdot \mathbf{r}_j} \right| \phi_{Pi} \right\rangle. \quad (5)$$

Equation (4) defines what is called the *dynamic charge*. Note that, when $K \rightarrow 0$, $q_K \rightarrow Z_p - N$, whereas $K \rightarrow \infty$ implies $q_K \rightarrow Z_p$. Therefore, if we choose $Z_p^{\text{eff}} = q_K$ within the CDW-EIS model, we will be taking into account the distortions of the projectile whenever the screening is not fully achieved. In particular, by the use of this dynamic charge for neutral projectiles we may recover a two-center description of the collision.

In the *prior* version of the transition amplitude,

$$a_{if}^-(\boldsymbol{\rho}) = -i \int_{-\infty}^{+\infty} \left\langle \chi_f^- \left| \left(H_{\text{el}} - i \frac{\partial}{\partial t} \right) \right| \chi_i^+ \right\rangle dt \quad (6)$$

where the operators act over the initial channel distorted-wave function, the V_T potential of (1) can be obtained by choosing a good description of the target bound state ψ_i in (2a). Such is the case of the Roothaan-Hartree-Fock wave functions [23]. Then, according to the work presented in [18,19,24], we may approximate V_P with a two-parameter Green-Sellin-Zachor (GSZ) [25–27] potential of the form

$$V_P(\mathbf{s}) = -\frac{q}{s} - \frac{1}{s}(Z_p - q)[H(e^{s/d} - 1) + 1]^{-1}, \quad (7)$$

where q is the asymptotic net charge and H and d are parameters that depend on Z_p and N [17,27]. Note that the first term of (7) is a long-range effective Coulomb interaction being solved by (3a) if $Z_p^{\text{eff}} = q$. In contrast, in order to include the previously presented dynamic charge q_K in the initial channel, i.e., to take $Z_p^{\text{eff}} = q_K$ in (3a), we must rearrange (7) as

$$V_P(\mathbf{s}) = -\frac{q_K}{s} - \frac{1}{s}(Z_p - q)\Omega(s) - \frac{q - q_K}{s}, \quad (8)$$

where $\Omega(s)$ is the GSZ screening function [27], corresponding to the factor in brackets in (7). Despite the fact that the potentials in (7) and (8) are essentially the same, the last term in (8) will contribute with an extra coherent term in the *prior* transition amplitude given by (6).

For completeness we have to mention that in order to approximate, to some extent, the target continuum state ψ_f in (2b) as a Coulombic continuum state the well-known Belkić [13] effective charge $Z_T^{\text{eff}} = n\sqrt{-2\varepsilon_i}$ was used. Note that ε_i is the energy of the orbital from where the active electron was emitted and n is its principal quantum number.

III. RESULTS AND DISCUSSION

A. Validity of the dynamic effective charge corrections

Given the projectile distortions shown in (3a) and (3b), it must be stated that four possible cases show up as we use a dynamic effective charge or an asymptotic one in each channel. However, as it can be seen in Fig. 1, not all the possibilities may lead to physically correct results. Before further discussion, let us clarify the notation. Throughout this paper we will be using ν to identify the initial channel and ξ for the final one; then, to indicate which effective charge was chosen for each channel we use the subscript “0” for the asymptotic net charge and “K” for the dynamic one.

Figure 1(a) shows the He target single ionization DDCS for the impact of a He^+ ion at 500 keV/u, for an emission angle of 15° . Meanwhile, Fig. 1(b) contains the total (target ionization plus projectile electron loss) single ionization DDCS at 15° for the 500-keV/u H atom impinging over He. As indicated, the different continuous curves stand for the different effective charge approaches.

Taking into account that high-energy electrons are mostly emitted in short-range [binary encounter (BE)] collisions, it must be expected that the target ionization DDCS for low Z_P dressed ions and their bare nucleus are practically the same. In fact, this is supported by [2,5] for the same collision systems considered in Fig. 1. Therefore, as neither of the results corresponding to $\nu_K\xi_K$ or $\nu_K\xi_0$ shows this physical behavior, we must discard them as a suitable approximation. In contrast, while the $\nu_0\xi_0$ DDCS underestimates the expected binary encounter peak in Fig. 1(a), it certainly does approach the expected bare-nucleus result in Fig. 1(b), for a neutral projectile. However, the best physical description is obtained considering the dynamic charge only in the final channel projectile distortion, i.e., in the $\nu_0\xi_K$ configuration.

The reason why the CDW-EIS *prior* calculations involving the dynamic charge in the initial channel, ν_K , do not lead to accurate results may lie in the asymptotic nature of the eikonal approximation. In fact, the asymptotic boundary conditions are no longer fulfilled in the *prior* formalism if the dynamic charge is used in the initial channel.

B. Target ionization by dressed ions

In Fig. 1(a), between 100 and 300 eV, the target ionization DDCS is higher when the dynamic charge is considered in

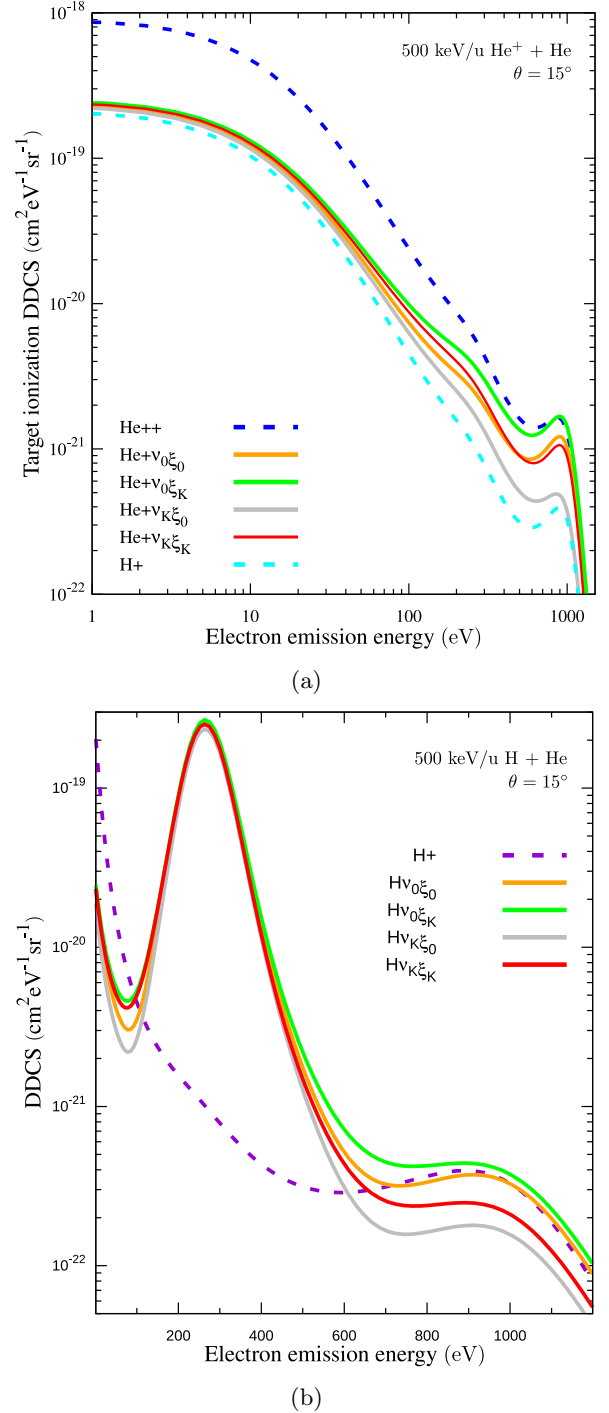


FIG. 1. Single ionization DDCS at $\theta = 15^\circ$ calculated for different charge corrections in comparison with bare projectiles. (a) He ionization by the impact of He^+ in comparison with same energy H^+ and He^{2+} impacts. (b) Electron emission for 500-keV/u $\text{H} + \text{He}$, in comparison with 500-keV/u $\text{H}^+ + \text{He}$. $\nu_0\xi_0$ stands for the use of the asymptotic charge in both channels; $\nu_0\xi_K$ means that the dynamic charge is applied in the final channel while the asymptotic one is used in the initial channel; $\nu_K\xi_0$ is exactly the opposite as the previous case and $\nu_K\xi_K$ indicates that the dynamic effective charge was included in both initial and final channels.

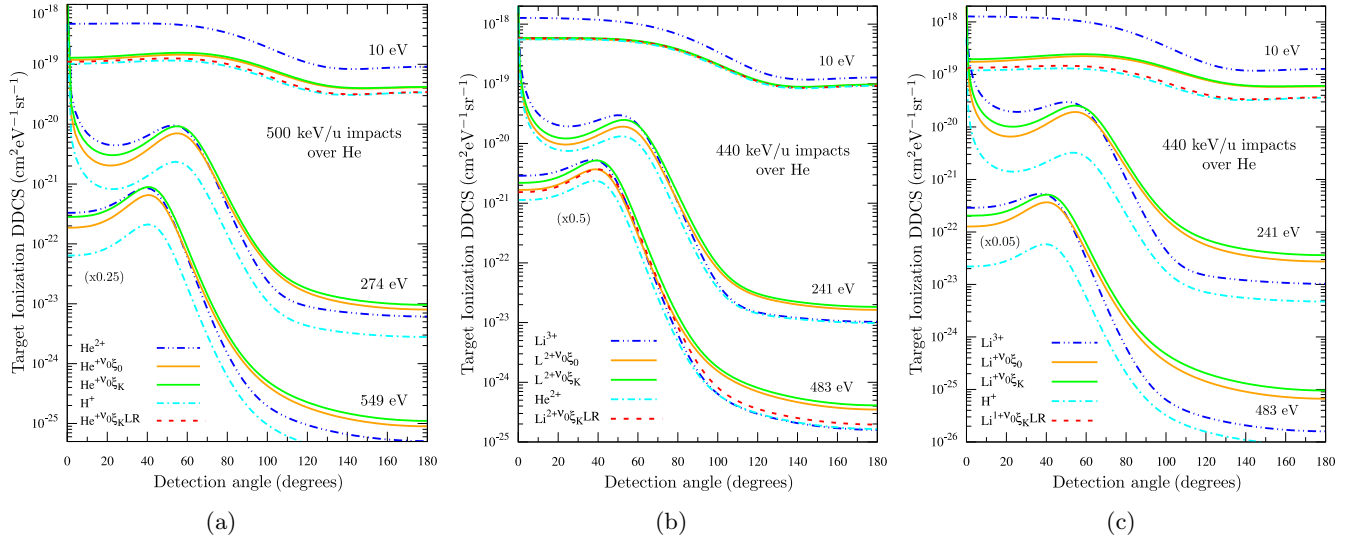


FIG. 2. He ionization DDCS as a function of the emission angle for fixed energies corresponding to soft collisions, the ECC cusp, and 45° binary encounter peak. Continuous lines are for dressed projectile impact, within the $\nu_0\xi_0$ or $\nu_0\xi_K$ cases (see Fig. 1 caption). Dashed lines are for bare projectile impacts. LR stands for the long-range interaction, i.e., the perturbation potential due to the short-range interaction is not taken into account.

the final channel (ξ_K). In particular, the electrons emitted at 270 eV have velocities similar to that of the projectile. Therefore, this increment in the DDCS is related to the well-known two-center emission effects [1]. In fact, the dynamic charge corresponding to these momentum transfers is higher than the asymptotic one, so it is expectable that ξ_K will produce an increase of the two-center effects, in comparison with ξ_0 .

In Fig. 1(a), electrons with high emission energy, around 950 eV, are emitted by close encounter (low impact parameter) binary collisions. It is reasonable to expect that in these conditions the reaction is mainly determined by the unscreened projectile nuclear charge. Regarding this, it can be seen that the $\nu_0\xi_K$ case is the only one that is consistent with the bare-projectile predictions.

At low emission energy, where the momentum transfer is not so high, the screening is complete and all the theoretical calculations corresponding to dressed projectiles are practically equivalent among themselves. Nevertheless, as it can be seen in Fig. 1(b), our calculations for the neutral H projectile at low energies lie below the H^+ single ionization DDCS. Although it seems to be reasonable, this is not what DuBois and Manson [2] found for the same system. In their work they explain that under certain momentum transfer threshold two-electron reactions may become more important contributing significantly to the low-energy electron emission, as, for example, target ionization with projectile excitation.

Despite the fact that we only deal with one active electron at a time, we do have a low-energy contribution derived from the presence of the projectile bounded electrons. In Fig. 2 the He target ionization DDCS as a function of the emission angle is shown for the impact of 500-keV/u He^+ in Fig. 2(a), 440-keV/u Li^{2+} in Fig. 2(b), and 440-keV/u Li^+ in Fig. 2(c). In each figure, three characteristic electron emission energies were chosen corresponding to the soft collisions, the electron capture to the continuum, and the binary encounter peak at

45° . In particular, for the fixed energy of 10 eV in Figs. 2(a) and 2(c) we find that both $\nu_0\xi_0$ and $\nu_0\xi_K$ calculations for Li^+ do not tend to the corresponding charge-like nucleus H^+ unless we discard the short-range potential (thus obtaining the dashed “LR” curves denoting long-range interaction). This shows that the actual short-range mono-electronic interaction is able to contribute to the low-energy electron emission. In addition, since the momentum transferred to these electrons is not so high, both asymptotic and dynamic charges corrections produce similar distortions.

Another interesting behavior is seen at backward angles in Fig. 2(b). There, the He target ionization DDCS is the same for both He^{2+} and Li^{3+} bare projectiles. This is a known saturation effect where after a certain charge threshold, for a given impact velocity, the DDCS will no longer increase with increasing Z_p [1]. However, as it can be seen, our calculations for dressed projectiles exceed the saturated target ionization DDCS, and this is due to the short-range interaction. By calculating the ionization achieved only by the long-range interaction (the dashed 483-eV “ $Li^{2+} \nu_0\xi_K$ LR” curve), we practically retrieve the saturated DDCS value.

Actually, the increments achieved with the screened potential (7) are due to the so-called antiscreening effect. When screened, the shape of the potential has a more rapid change in shape, over a certain region, than the Coulombic one. Therefore, the gradient is larger and so a greater force is exerted over the active bound electron [28]. However, this may not be the only antiscreening mechanism leading to DDCS enhancements. In Fig. 2(b), at forward emission angles and high energies (483 eV), a notorious DDCS increment due to the final channel charge correction can be seen. By the equality between the $Li^{2+} \nu_0\xi_K$ LR and $Li^{2+} \nu_0\xi_0$ results we can state that the increment in $Li^{2+} \nu_0\xi_K$ is achieved by the dynamic charge correction. This region of the spectrum corresponds to the binary encounter emission, and similar

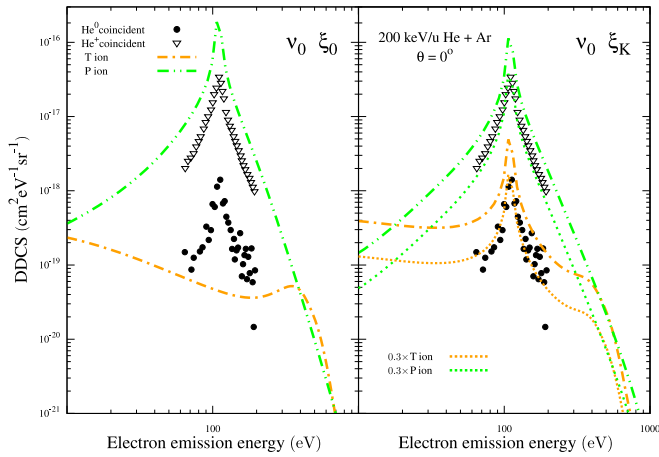


FIG. 3. Theoretical and experimental results for 200-keV/u He + Ar at 0° . “T ion” and “P ion” are our calculated target ionization and projectile electron loss, respectively. In panel (a) all calculations are for the $\nu_0\xi_0$ case while in panel (b) all calculations are for the $\nu_0\xi_K$ one. The experimental results are from [11]. Dotted lines are both multiplied by a factor of 0.3 to fit experiments.

enhancements are seen in Figs. 1, 5(a), and 5(b). These results may be explained by another possible antiscreening mechanism called secondary electron scattering [29]. In such a process, the projectile electrons interact with the active one, which is already in its continuum state after a close encounter ionization process, altering its trajectory and thus deflecting it to forward angles with high energy. In the present model, the projectile electronic structure affects the interaction between the active electron and the projectile through the effective dynamic charge. Being considered in the final channel distortion, this charge does influence the active electron continuum state evolution. Also, the interaction becomes stronger as the momentum transfer increases, thereby leading to an enhancement of the DDCS over the binary encounter peak region of the spectrum.

C. Two-center emission effects with neutral projectiles

As mentioned earlier, by using the asymptotic net charge in the case of a neutral projectile, the distortions will vanish and the CDW-EIS model will reduce to a single center description. In contrast, using instead the dynamic charge in the final channel distortions we can recover a two-center description wherever the projectile nuclear field is not fully screened.

In Fig. 3, the target and projectile single ionization DDCSs for 200-keV/u He impinging on Ar are plotted, in the target reference frame, as a function of the emitted electron energy at a fixed angle of 0° . On the left we have the $\nu_0\xi_0$ results while on the right we have those for $\nu_0\xi_K$. Along with the CDW-EIS calculations, experimental data from [11] are plotted. These data allow a comparison with direct measurements of the ECC and the electron loss to the continuum (ELC) peaks, each one corresponding to the detection of an electron in coincidence with He and He⁺ postcollisional projectile charge states, respectively. Thus, it can be seen that unlike the $\nu_0\xi_0$ case the target ionization spectrum gets peaked at around 110 eV for $\nu_0\xi_K$, i.e., when the final distortion does not vanish. The

electrons emitted at that energy have a velocity similar to that of the projectile, so the peak may be related to the ECC due to a postcollisional interaction between the active electron and the partially screened field of the neutral projectile. Precisely, the peak is originated by the divergence in the normalization factor of the projectile distortion in the final channel. Theoretical calculations and the direct ECC measurements are in good qualitative agreement, showing only a difference in magnitude.

As regards the projectile ionization peak, the comparison between experimental and theoretical results is also quite good. However, for the He projectile electron-loss calculation the collision system must be reversed to 200-keV/u Ar + He, and then the DDCS transformed from the He reference frame to the Ar (laboratory) one. Because of the high asymmetry between the He and Ar atoms, the collision energy for this inversed collision system may not fulfill the perturbative framework of the distorted-wave models, so the electron-loss calculations in Fig. 3 should be taken with caution.

In contrast, the projectile electron-loss calculations for 440-keV/u Li⁺ + He are by far more reliable and we can show that they also bring evidence about the ECC phenomena with neutral atomic projectiles. In Figs. 5(c) and 5(d) both $\nu_0\xi_0$ (left) and $\nu_0\xi_K$ (right) theoretical results are plotted against experimental data from [18], for emission angles of 120° and 170° . Among those calculations, for the projectile ionization DDCS, it can be seen that there is a great difference in magnitude and slope between 1- and 200-eV emission energy. In addition, the use of the dynamic charge in the final channel distortion at backward angles makes a significant contribution to the total DDCS, improving the agreement with the experimental data.

In order to search for the cause of the mentioned behavior in the projectile ionization DDCS in the $\nu_0\xi_K$ case, we analyzed the Lorentz transformations. We calculated the emission angle and energy, in the projectile reference frame, of the electrons detected at 170° and between 1 and 200 eV in the laboratory frame, taking into account the relative velocity between frames of 4.21 a.u. In Fig. 4(a), the emission angle and energy in the projectile reference frame are plotted as a function of the laboratory emission energy. It can be seen that the mentioned electrons were emitted in the projectile frame at angles ranging between 0° and 5° with emission energies between 250 and 800 eV. These results indicate that the electrons detected at backward angles and low energies in the laboratory frame came from a forward emission at velocities higher than the collision velocity in the projectile frame.

Actually, analyzing the inverted collision 440-keV/u He + Li⁺ system (the He target is now the projectile) at 5° in Fig. 4(b), we can state that the observed increment in magnitude in Fig. 5(d) is due to an electron capture to the continuum by the neutral He “projectile.” In addition, Fig. 4(a) shows that, as the laboratory emission energy decreases from 200 to 1 eV, so do the projectile frame emission angle and energy up to a minimum of 0° and 240 eV (electron velocities of 4.21 a.u.). Therefore, the change in slope in Fig. 5(d) as we move from 200 to 1 eV in the $\nu_0\xi_K$ case is caused by the increase of the ECC peak magnitude that occurs as the emission angle (in the projectile frame) tends to 0° .

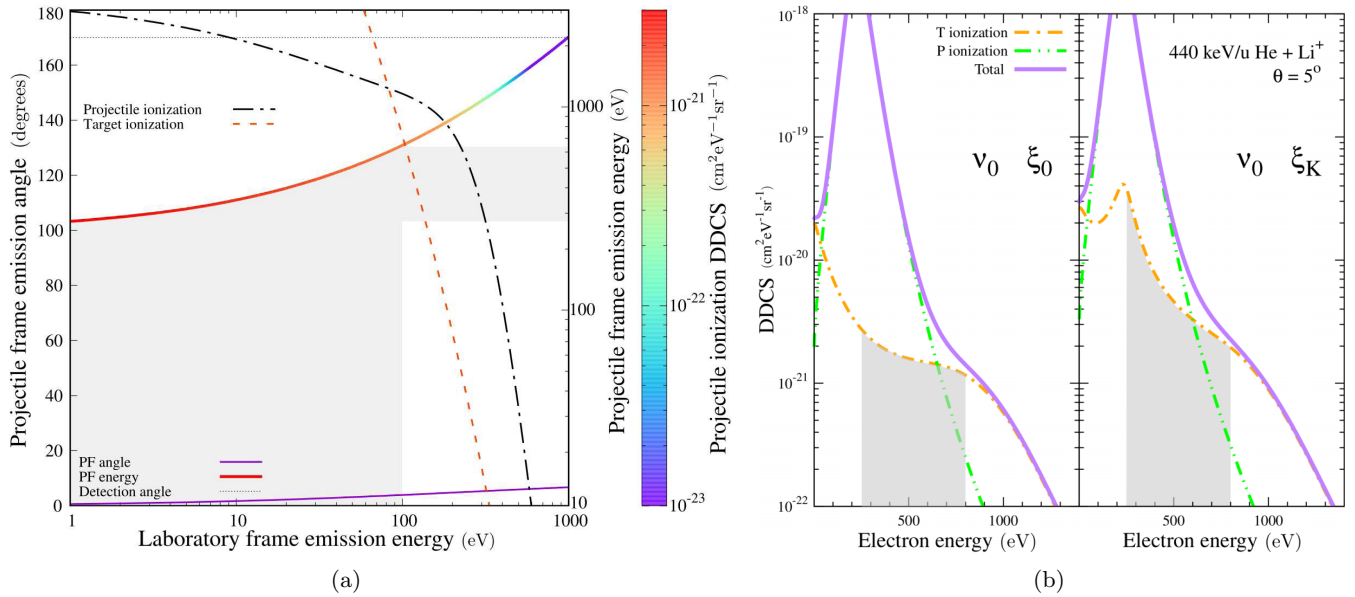


FIG. 4. Analysis of those electrons emitted from the projectile and detected in the laboratory frame at 170° with energy from 1 to 100 eV. (a) Energy and emission-angle Lorentz transformations from the laboratory frame to the projectile one as a function of the detected energy. Contained in the projectile frame emission energy curve is the value of the projectile ionization DDCS at that energy. (b) Target and projectile ionization DDCS for the reversed collision system of Fig. 5(d), 440-keV/u He + Li^+ , at 5° .

D. Results for 440-keV/u Li^+ + He

In Fig. 5 the theoretical CDW-EIS *prior* single ionization DDCS calculations for $\nu_0\xi_0$ (left) and $\nu_0\xi_K$ (right) are plotted along with experimental data from [18]. From Figs. 5(a)–5(d) the fixed emission angles range between 10° and 170° . The sharp structure at about 550 eV in Fig. 5(a) is related to the Li^+ autoionization [18] and therefore cannot be predicted by our theoretical model. As seen for the contrast against experimental data, an overall better agreement is achieved with the $\nu_0\xi_K$ calculations rather than the $\nu_0\xi_0$ case. This encourages us to think that a more realistic collision description for dressed ions and neutral atomic projectiles is obtained by the inclusion of the dynamic effective charge in our analytical framework. For backscatter emission angles [Figs. 5(c) and 5(d)], for emission energies larger than 100 eV, the major contribution to electron emission comes from the projectile electron loss, which is driven by the neutral atomic target distortions in the projectile frame calculations, as we showed above.

IV. CONCLUSIONS

We have investigated theoretically the electron emission in collisions between atomic targets and dressed projectiles within the framework of the CDW-EIS *prior* model. A dynamic effective charge as a function of the momentum transfer was proposed so as to have an analytical final-channel distortion that takes into account the dynamic screening of the dressed projectile. Actually, the calculations with this dynamic charge ($\nu_0\xi_K$) and those with an asymptotic one ($\nu_0\xi_0$) are the same at low emission energies. However, as the emission energy increases, the $\nu_0\xi_K$ ionization DDCS is enhanced with respect to the $\nu_0\xi_0$ results. In particular, for low Z_P dressed projectiles, the $\nu_0\xi_K$ results at binary encounter emission energies are similar to those obtained for

the corresponding bare projectile. In fact, under the validity of the straight-line impact parameter approximation, the close encounter nature of those collisions implies that the projectile nuclear charge might not be completely screened by its bounded electrons and therefore a more realistic final distortion is obtained by using the dynamic effective charge.

Taking the BE peak as a reference, we found that initial channel distortions should keep the usual asymptotic net charge because the use of the dynamic one instead does not lead to the correct amplitude result of the BE peak. Furthermore, the use of a close encounter effective screening model in the initial channel distortion along with the asymptotic eikonal approximation is basically a contradiction.

We also analyzed our calculations for the $\nu_0\xi_0$ and $\nu_0\xi_K$ cases throughout all the emission angles for three characteristic electron energies. At low emission energies (10 eV) we showed that both calculations lead to the same results as expected [5] from the equality between the dynamic charge and the net one for low momentum transfer collisions. Then, for higher momentum transfers the difference between $\nu_0\xi_0$ and $\nu_0\xi_K$ cases increases, the latter holding higher DDCS values, especially at forward emission angles, which means that postcollisional two-center effects are stronger due to a higher effective charge being considered. At backward emission angles and high emission energies, a great difference exists between the dressed projectiles and the bare ones. In particular, despite the fact that the ionization of He by the impact of He^{2+} and Li^{3+} at 440 keV/u shows clear saturation effects for backscattering angles, the target ionization DDCS for dressed Li^{2+} projectiles is higher than the saturated ones. This increment, as shown, is due to the short-range perturbation potential. In addition, the same short-range interaction prevents the low-energy He ionization DDCS by dressed He^+ and Li^+ projectiles from behaving as the corresponding

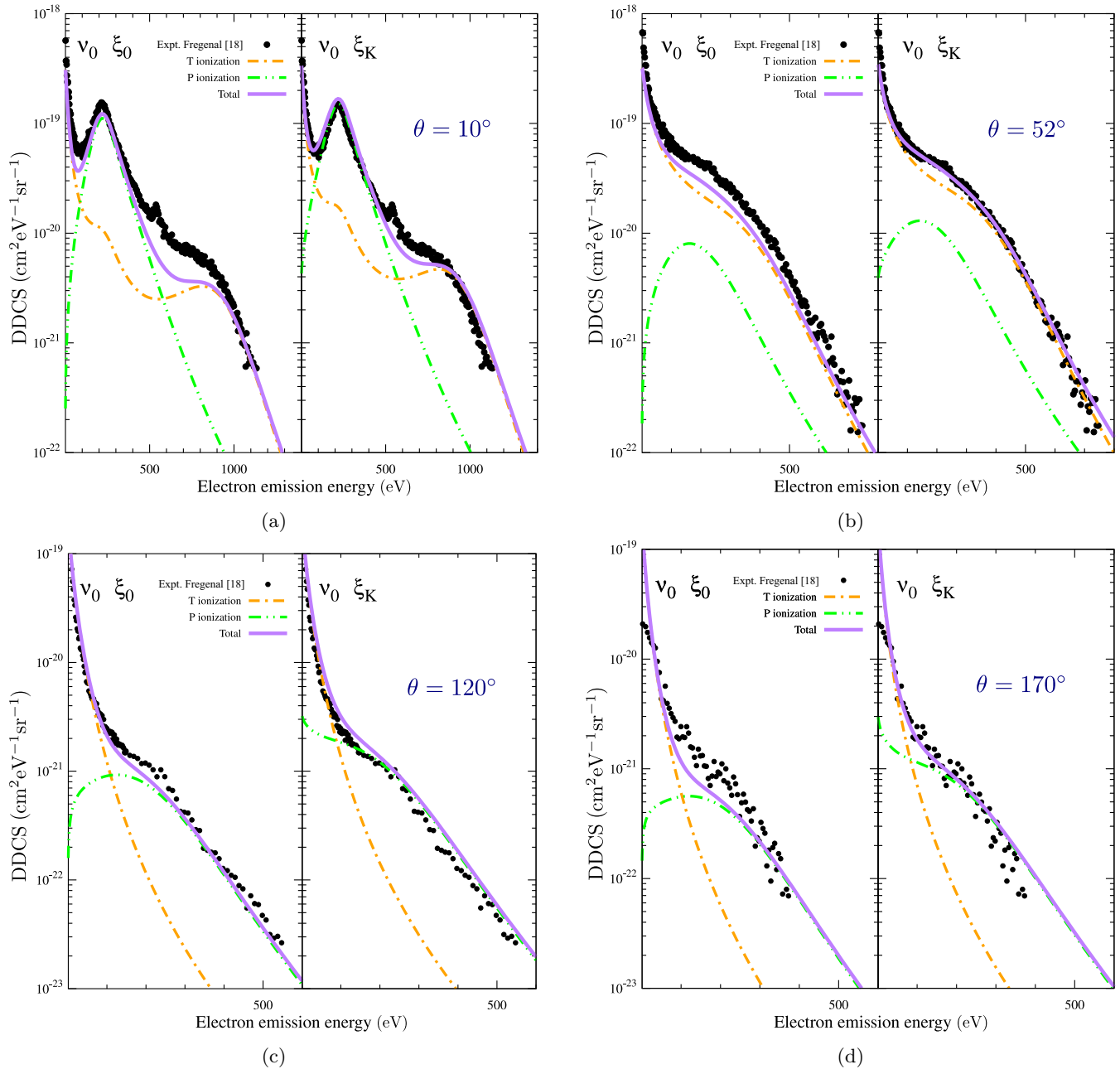


FIG. 5. Experimental and theoretical DDCS for 440-keV $\text{Li}^+ + \text{He}$ at fixed emission angles of (a) 10° , (b) 52° , (c) 120° , and (d) 170° . On the left panel of each figure the calculations use the asymptotic net charge in both initial and final channel, $\nu_0 \xi_0$, while in the right panel we have the $\nu_0 \xi_K$ case, i.e., a net charge in the initial channel distortion and a dynamic effective charge in the final channel distortion. Experimental data are from [18].

results obtained for the asymptotic equivalent H^+ bare projectile. In other words, the short-range projectile potential acts as another mechanism for the electron emission, allowing further ionization where long-range interaction gets saturated and also contributing to low-energy emission, like the dielectronic contribution calculated among other theoretical approaches [2].

Additionally, in comparison with experimental data from [18], a significant contribution of the ECC happening in the projectile reference frame was found in the electronic spectrum measurements for backward angles in the laboratory

system. As long as the projectile electron loss is produced by the distortion of the neutral target, this finding may suggest that a dynamic screening for neutral atoms is worth considering at least for the sake of simplicity provided by analytical expressions. For example, Macri and Barrachina [10] have shown that the ECC cusp in the 200-keV/u $\text{He} + \text{Ar}$ system is affected by the presence of metastable $\text{He}(2S^1)$ projectiles. In the present paper, we obtained a good qualitative agreement with the same experimental data by considering a partially screened field of a ground-state He projectile instead. Additionally, by multiplying the target and projectile ionization

DDCS by a factor of 0.3, it can be seen that the shapes of ECC and ELC peaks are well described with only a difference in magnitude. To this matter, predictions by the present model for the ECC peak in neutral projectile collisions and its relation with metastable states of the projectile (see [30,31]) will be further investigated.

Finally, the consideration of a dynamic effective charge in the final channel distortion leads to small overall improvements for projectiles with high ionization degree, e.g., Li^{2+} ,

but it can also be a major correction to the model for those projectiles with low or zero ionization degree.

ACKNOWLEDGMENTS

The authors acknowledge financial support of the Consejo Nacional de Investigaciones Científicas y Técnicas de la República Argentina through the Project PICT 2015-3392.

-
- [1] N. Stolterfoht, R. D. DuBois, R. DuBois, and R. D. Rivarola, *Electron Emission in Heavy Ion-Atom Collisions*, Springer Series on Atoms and Plasmas Vol. 20 (Springer, New York, 1997).
- [2] R. D. DuBois and S. T. Manson, *Nucl. Instrum. Methods Phys. Res. Sect. B* **86**, 161 (1994).
- [3] R. D. DuBois and S. T. Manson, *Phys. Rev. A* **42**, 1222 (1990).
- [4] J. H. McGuire, N. Stolterfoht, and P. R. Simony, *Phys. Rev. A* **24**, 97 (1981).
- [5] S. T. Manson and L. H. Toburen, *Phys. Rev. Lett.* **46**, 529 (1981).
- [6] C. R. Garibotti and R. O. Barrachina, *Phys. Rev. A* **28**, 2792 (1983).
- [7] L. Sarkadi, J. Pálinkás, A. Kövér, D. Berényi, and T. Vajnai, *Phys. Rev. Lett.* **62**, 527 (1989).
- [8] D. H. Jakubaša-Amundsen, *J. Phys. B* **22**, 3989 (1989).
- [9] R. O. Barrachina, *J. Phys. B* **23**, 2321 (1990).
- [10] P. A. Macri and R. O. Barrachina, *J. Phys. B* **31**, 1303 (1998).
- [11] H. Trabold, G. M. Sigaud, D. H. Jakubassa-Amundsen, M. Kuzel, O. Heil, and K. O. Groeneveld, *Phys. Rev. A* **46**, 1270 (1992).
- [12] A. Báder, L. Sarkadi, L. Víkor, M. Kuzel, P. A. Závodszky, T. Jalowy, K. O. Groeneveld, P. A. Macri, and R. O. Barrachina, *Phys. Rev. A* **55**, R14 (1997).
- [13] D. Belkić, *J. Phys. B* **11**, 3529 (1978).
- [14] D. S. F. Crothers and J. F. McCann, *J. Phys. B* **16**, 3229 (1983).
- [15] P. D. Fainstein, V. H. Ponce, and R. D. Rivarola, *J. Phys. B* **24**, 3091 (1991).
- [16] J. M. Monti, R. D. Rivarola, and P. D. Fainstein, *J. Phys. B* **41**, 201001 (2008).
- [17] J. M. Monti, R. D. Rivarola, and P. D. Fainstein, *J. Phys. B* **44**, 195206 (2011).
- [18] D. Fregenal, J. M. Monti, J. Fiol, P. D. Fainstein, R. D. Rivarola, G. Bernardi, and S. Suárez, *J. Phys. B* **47**, 155204 (2014).
- [19] P. M. Hillenbrand, S. Hagmann, J. M. Monti, R. D. Rivarola, K. H. Blumenhagen, C. Brandau, W. Chen, R. D. DuBois, A. Gumberidze, D. L. Guo, M. Lestinsky, Y. A. Litvinov, A. Müller, S. Schippers, U. Spillmann, S. Trotsenko, G. Weber, and T. Stöhlker, *Phys. Rev. A* **93**, 042709 (2016).
- [20] P. D. Fainstein, V. H. Ponce, and R. D. Rivarola, *J. Phys. B* **21**, 287 (1988).
- [21] J. M. Monti, M. A. Quinto, and R. D. Rivarola, *Atoms* **9**, 3 (2021).
- [22] I. A. Sellin, *Structure and Collisions of Ions and Atoms* (Springer-Verlag, Berlin, 1978).
- [23] E. Clementi and C. Roetti, *At. Data Nucl. Data Tables* **14**, 177 (1974).
- [24] L. H. Toburen, R. D. DuBois, C. O. Reinhold, D. R. Schultz, and R. E. Olson, *Phys. Rev. A* **42**, 5338 (1990).
- [25] A. E. Green, D. L. Sellin, and A. S. Zachor, *Phys. Rev.* **184**, 1 (1969).
- [26] P. P. Szydlík and A. E. Green, *Phys. Rev. A* **9**, 1885 (1974).
- [27] R. H. Garvey, C. H. Jackman, and A. E. S. Green, *Phys. Rev. A* **12**, 1144 (1975).
- [28] L. Végh and L. Sarkadi, *J. Phys. B* **16**, L727 (1983).
- [29] P. Richards, D.-H. Lee, T. Zouros, J. Sanders, and J. Shinpaugh, *J. Phys. B* **23**, L213 (1990).
- [30] L. Víkor, L. Sarkadi, F. Penent, A. Báder, and J. Pálinkás, *Phys. Rev. A* **54**, 2161 (1996).
- [31] L. Víkor and L. Sarkadi, *Phys. Rev. A* **55**, R2519 (1997).